Analysis of atmospheric aerosol properties using lidar measurements and their impact on radiative budget in Barcelona over the past 20 years

Simone Lolli[a,b*], Michaël Sicard[c,b], Adolfo Comerón[b], Cristina Gil-Díaz[b], Daniel Camilo Dos Santos Oliveira[b], Tony C. Landi[d], Alejandro Rodríguez-Gómez[b], Constantino Munoz-Porcar[b], Francesc Rocadenbosch[b,e], Federico Dios[b]

[a]Italian National Research Council CNR-IMAA, 85050 Tito Scalo (PZ), Italy; [b]CommSensLab, Dept. of Signal Theory and Communications, Universitat Politènica de Catalunya, 08034 Barcelona, Spain; [c]Lab. de l'Atmosphère et des Cyclones, Univ. de La Réunion, 97744, Saint Denis, France;[d]CNR-ISAC, Via Gobetti 101, 40129, Bologna, Italy; [e]Institut d'Estudis Espacials de Catalunya, 08034 Barcelona, Spain

ABSTRACT

Aerosols are significant atmospheric constituents that modulate radiation and cloud processes. We evaluated 17-year aerosol profile trends in Barcelona, Spain, from lidar measurements. In summer aerosol reaches 5 km, while in the other seasons it exhibits clear exponential decay. Sahara dust transport affects all seasons, with winter layers above and others penetrating the boundary layer. This study informs the formation of haze and urban preservation strategies in the Mediterranean. The analysis puts in evidence that the averaged net radiative effect is of cooling at both surface level and top of the atmosphere.

Keywords: Aerosol profiles, Lidar Remote Sensing, Aerosol Radiative Effects, Air Quality

1 INTRODUCTION

Aerosols have a major influence on human health,[1–3] environment,[4, 5] and climate.[6] Their transient nature, which spans several days to weeks, makes them potent drivers of climate and air quality dynamics. Derived from various sources, from natural phenomena, such as dust[7] and sea salt, to human activities, such as combustion and industrial operations, their impact encompasses human health, urban heat modulation, and climate modulation. In urban settings, aerosols significantly shape the effect of urban heat islands, particularly during heat waves.[8–10] In addition, their climatic repercussions are multifaceted. Aerosols scatter and absorb solar radiation, affecting the Earth's energy balance and generating cooling or warming effects.[11] The interplay of aerosol emissions, composition, and climate has considerable implications and even influences atmospheric stability, circulation, and precipitation.[12,13] Importantly, these aerosols significantly alter the radiative forcing, resulting in a negative effective radiative forcing of -1.3 W/m^2 in the industrial era. Despite advancements in assessing aerosol effects, challenges remain in emission databases, particularly for absorbing aerosols such as biomass burning and dust. A proposed[1] top-down approach suggests higher emission values than traditional methodologies, hinting at the potential significance of such data. To dissect these complexities, our study combines comprehensive lidar data from the EARLINET/ACTRIS research infrastructure[14,15] to assess changes in aerosol properties over the past 17 years in Barcelona, Spain. In the context of an evolving Mediterranean climate and impending ecological changes, this research has far-reaching implications, potentially illuminating the role of aerosols in offsetting climate change and inform future adaptation strategies.

2 METHODOLOGY

2.1 Lidar

Lidar, an optically active remote sensing technique that uses a laser[16] as a source, has gained prominence in atmospheric research. It provides essential information about the vertical distribution of aerosols, clouds, and gas properties,

* E-mail: simone.lolli@upc.edu

Simone Lolli, Michaël Sicard, Adolfo Comerón, Cristina Gil-Díaz, Daniel Camilo Dos Santos Oliveira, Tony C. Landi, Alejandro Rodríguez-Gómez, Constantino Munoz-Porcar, Francesc Rocadenbosch, and Federico Dios "Analysis of atmospheric aerosol properties using lidar measurements and their impact on radiative budget in Barcelona over the past 20 years", Proc. SPIE 12730, Remote Sensing of Clouds and the Atmosphere XXVIII, 1273007 (19 October 2023) https://doi.org/10.1117/12.2685167

including their optical and microphysical characteristics. Applied in various atmospheric studies, from air quality monitoring to cloud structure analysis, and even greenhouse gas measurements, lidar offers high vertical and temporal resolution for regional and local-scale investigations. Different lidar techniques, such as elastic,[17,18] Raman, Dial, Doppler, and high spectral resolution laser (HSRL), cater to diverse assumptions, allowing property retrieval with varying precision.

Within the EARLINET/ACTRIS research infrastructure, aerosol lidar observations are accessible, among them those of the multiwavelength Raman lidar at Universitat Politècnica de Catalunya (UPC). The system is equipped with an Nd:YAG laser source with second- and third-harmonic generators. In its current status, it is the third embodiment of the Barcelona EARLINET lidar station, with eight receiving channels in an elastic/Raman aerosol/water-vapor configuration. It transmits pulses at 1064-nm (NIR), 532-nm (visible), and 355 nm (UV) wavelengths, and receives three elastic, three Raman (one for water vapor), and two depolarization channels. This enables aerosol profiling at three key harmonics: 355, 532, and 1064 nm, further enhancing the versatility of the lidar system.

2.2 Fu-Liou-Gu Radiative Transfer Model

The Fu-Liou-Gu (FLG) radiative transfer model[19,20] is a well-established tool commonly utilized to simulate radiative processes in the atmosphere of the Earth. While primarily developed for satellite and ground-based radiometric observations, its application has extended using lidar measurements as input. The FLG model enables the assessment of radiative fluxes and heating rates to assess the radiative budget of the atmosphere-Earth system.

The FLG model incorporates scattering and absorption processes to simulate the interaction of light with atmospheric particles and gases. In our study, we used the aerosol optical properties recovered by UPC lidar as input for computations.

2.3 Long-term seasonal lidar observations

Quantifying seasonal variability in vertically resolved optical properties retrieved by lidar observations remains crucial from a climatological perspective. To address this, we divided the year into four seasons: December-January-February (DJF), March-April-May (MAM), June-July-August (JJA), and September-October-November (SON). Averaged profiles for each season were obtained by calculating the median of level 2 backscattering atmospheric profiles from UPC lidar, mitigating outlier effects. For the period 2004 to 2020, quality-assured lidar aerosol backscatter profiles totaled 2630 at 532 nm. While cloud cover and adverse weather conditions led to fewer backscatter profiles in fall and winter, spring and summer exhibited higher average profiles.

3 RESULTS

3.1 Geometrical analysis and suggestions

The corresponding median average profiles, displayed in Figure 1 with relative accuracy, highlight the distinctions between seasons. In particular, the summer aerosol layer, which decreased sharply in the first km, extended to 5 km in altitude. In contrast, backscatter profiles during spring, fall, and winter exhibited a more pronounced exponential decline. Consistent steep drop during winter up to 1.7 km indicated locally sourced aerosols, while other profiles suggested elevated boundary layer heights or upper air aerosol transport, particularly prevalent during summer months.

During the months of June, July, and August, the aerosol backscatter profile indicates that aerosol loading during this season extends to 5 km. On the contrary, the backscatter profile for winter, which includes lidar observations in December, January, and February, shows a steep exponential decline, with aerosols absent beyond 2.5 km. For spring (March, April, May) and fall (September, October, November), the aerosol backscatter profiles also exhibit exponential decay patterns, although with elongated tails indicating aerosol presence up to 3 km in both cases. Spring, fall and, in particular, winter profiles can be accurately described by exponential curves fall and, particularly, a relative scale height denoted as H.

As an example, during winter, a scale height of H=0.61 km implies that around 63% of the aerosol load is confined below this height. We considered upper transport due to dust outbreaks, while aerosols from surface up to 1.7 Km are considered local urban background.

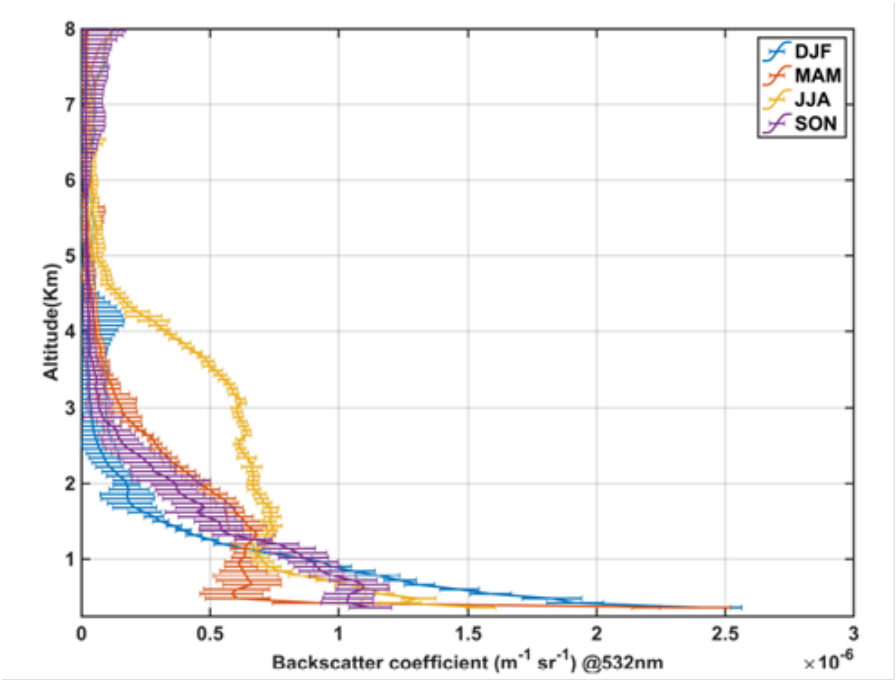

Figure 1. Vertically resolved median backscattering profiles for DJF, MAM, JJA, and SON. Error bars are obtained by computing the standard error. The spatial resolution is a constant and fixed at 60 m.

3.2 Radiative effects.

We also analyzed the radiative effects based on the seasonal averaged bakcscattering profiles We considered an urban environment with a surface albedo of 0.12. We computed the heating rate (K/day) at noon for each central month of the four seasons, i.e., January, April, July, and October, transforming the backscattering profile into optical depth, using a lidar ratio if 50sr for dust particles and 70sr for polluted environment particles. We report the results of the FLG calculations in Figure 2. The heating rate profiles show general atmospheric heating, which more or less follows the backscattering profile. In Table 1, we also report the radiative effects at the top of the atmosphere (TOA) and the surface (SFC), respectively.

The atmospheric energy budget (ATM) is the difference between the TOA and surface energy budgets; it represents the energy that is exchanged between the surface and the atmosphere, and it reflects the impact of atmospheric processes on the surface energy budget.

3.3 Trends

The Mann-Kendall[21] analysis of seasonal averages applied to the integrated backscatter coefficient (units sr^{-1}) did not reveal any significant trend in the boundary layer over the studied period. However, a small increase of this parameter in the 3 km – 8 km height of 5.48×10^{-8} sr^{-1} $year^{-1}$ (fig. 3) seems to indicate an increase of aerosols advected in the free troposphere from distant sources (biomass burning and dust outbreaks).

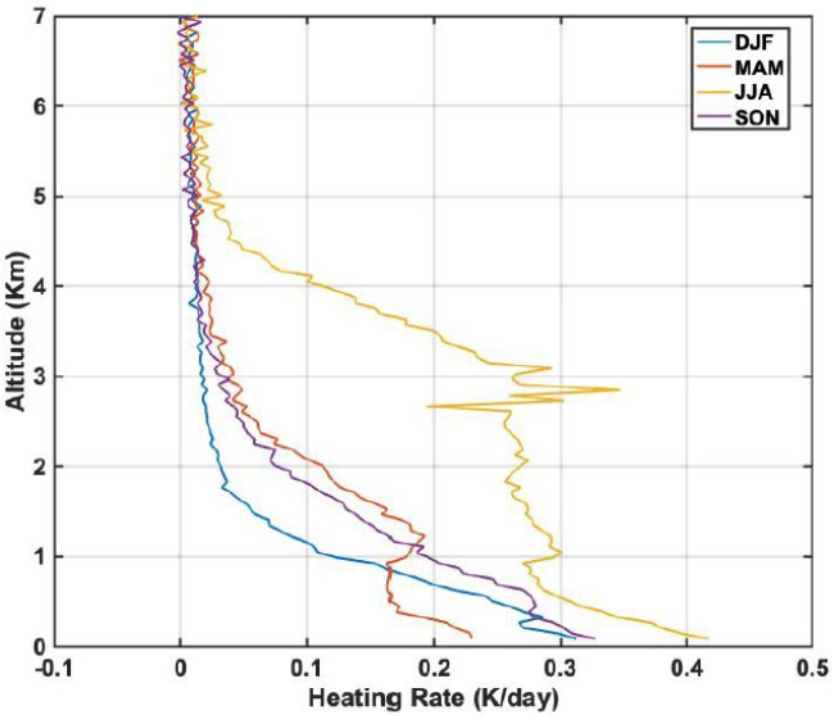

Figure 2. Vertically resolved median Heating Rate profiles for DJF, MAM, JJA, and SON.

Table 1. Net radiative effect of seasonal averaged atmospheric aerosols

Season	SFC (W/m^2)	TOA (W/m^2)	ATM (W/m^2)
DJF	-12.2	-8.8	3.4
MAM	-13.0	-7.9	5.1
JJA	-25.4	-13.1	12.3
SON	-14.9	-8.1	6.8

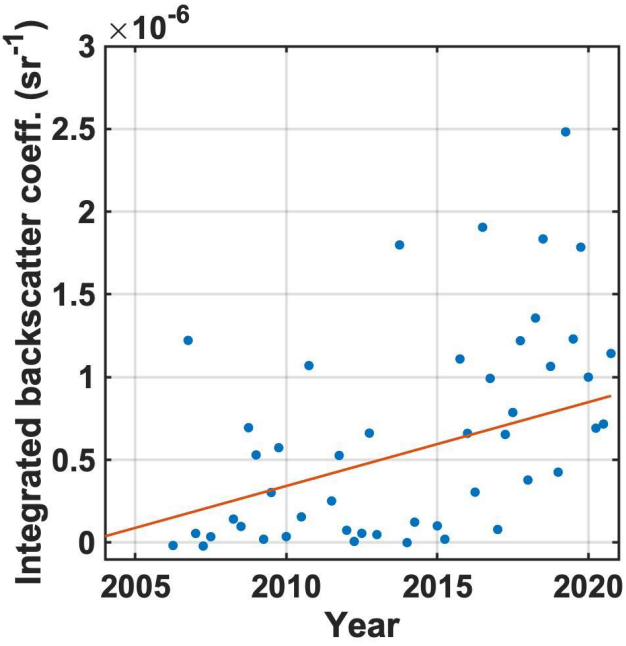

Figure 3. Sen's slope for the seasonal integrated-backscatter median profiles in the range 3 km – 8 km between 2004 and 2020.

4 CONCLUSIONS

This paper has presented a preliminary exploitation of the long-term database of lidar profiles obtained by the EARLINET/ACTRIS Barcelona station from 2004 to 2020. It sets the framework of further analyses that can be carried on data from this station and of all the EARLINET/ACTRIS stations in general, whose data are publicly available at https://www.earlinet.org/index.php?id=125 and at the general ACTRIS data portal (https://www.actris.eu/topical-centre/data-centre), where data on aerosol in situ measurements, as well as on clouds and trace gases, obtained by both in situ and remote sensing techniques, are also found. These data provide information useful for all the time scales, from events affecting air quality to assessing climate trends.

The lidar data of the Barcelona station show a clear difference in the median backscatter coefficient profiles at 532 nm between the summer months and the rest of the year. In summer the median profile show aerosols up to 5 km, with a center of mass around 2.5 km. Median profiles for the other seasons can be well approximated by exponential decays with different scales. Dust outbreaks float over the boundary layer in winter time, while they can be embedded in it in the other seasons. No noticeable trend of the integrated backscatter profiles is found in the boundary layer, but a small increasing trend of 5.48×10^{-8} sr^{-1} $year^{-1}$ is revealed in the 3 km – 8km range for the studied time period, possibly indicating increased occurrence of long-range aerosol advections.

A first approach to the aerosol radiative effects at noon for the central month of each season has also been performed using the Fu-Liou-Gu radiative transfer model.

ACKNOWLEDGEMENTS

This work has been made possible through the efforts of many people, whom it would be too long to mention, and the funding of many grants through the years, in particular European projects of different framework programmes (FP5 EARLINET project (ID EVR1-CT-1999-40003), FP6 EARLINET-ASOS (ID: 25991), FP7 ACTRIS (ID: 262254), H2020 ACTRIS-2 (ID: 654109), ACTRIS-PPP (ID: 739530), ACTRIS IMP (ID: 871115) and ATMO-ACCESS (ID: 101008004)), projects of the Spanish National Research Programmes (refs. TIC 431/93, AMB96-1144-C02-01, REN2000-1907-CE, REN2000-1754-C02-02 / CLI, REN2003-09753-C02-C02 / CLI, REN2003-09753-C02-C CGL2008-01330-E/CLI 02 / CLI, REN2002-12784-E, CGL2005-5131-E, CGL2006-27108-E/CLI, CGL2006-26149-E/CLI, CGL2007-28871-/CLI, CTM2006-27154-E/TECNO, TEC2006-07850/TCM, TEC2009-09106, TEC2012-34575,

TEC2015-63832-P and PID2019-103886RB-I00), the project of the Catalan Regional Government IMMPACTE, and the ESA project No. nº 21487/08/NL/HE. The support of the European Union through NextGenerationEU funds is also gratefully acknowledged.

REFERENCES

[1] Lolli, S., Chen, Y.-C., Wang, S.-H., and Vivone, G., "Impact of meteorological conditions and air pollution on COVID-19 pandemic transmission in Italy," Scientific Reports **10** (1), 1–15 (2020), https://doi.org/10.1038/s41598-020-73197-8.

[2] Lolli, S. and Vivone, G., "The role of tropospheric ozone in flagging COVID-19 pandemic transmission," Bulletin of Atmospheric Science and Technology, 1–5 (2020), doi: 10.1007/s42865-020-00026-1.

[3] Lolli, S., Piazza, F., and Vivone, G., "Government restriction efficiency on curbing COVID-19 pandemic transmission in Western Europe," COVID **3**(8), 1079–1091 (2023), https://doi.org/10.3390/covid3080079.

[4] Lolli, S., Khor, W. Y., M. Z. Matjafri, M., and Lim, H. S., "Monsoon season quantitative assessment of biomass burning clear-sky aerosol radiative effect at surface by ground-based lidar observations in Pulau Pinang, Malaysia in 2014," Remote Sensing **11**(22) (2019), https://doi.org/10.3390/rs11222660.

[5] Lolli, S., "Is the air too polluted for outdoor activities? Check by using your photovoltaic system as an air-quality monitoring device," Sensors **21**(19) (2021) https://doi.org/10.3390/s21196342.

[6] Lolli, S., Vivone, G., Lewis, J., Sicard, M., Welton, E., Campbell, J., Comerón, A., D'Adderio, L., Tokay, A., Giunta, A., and Pappalardo, G., "Overview of the new version 3 NASA Micro-Pulse Nework (MPLNET) Automatic Precipitation Detection Algorithm," Remote Sensing **12**(71) (2020), doi:10.3390/rs12010071.

[7] Landi, T. C., Bonasoni, P., Brunetti, M., Campbell, J. R., Marquis, J. W., Di Girolamo, P., and Lolli, S., "Aerosol direct radiative effects under cloud-free conditions over highly-polluted areas in Europe and Mediterranean: A ten-years analysis (2007–2016)," Remote Sensing **13**(15), 2933 (2021), https://doi.org/10.3390/rs13152933.

[8] Bilal, M., Nichol, J., Nazeer, M., Shi, Y., Wang, L., Kumar, K., Ho, H.C.and Mazhar, U., Bleiweiss, M., Qiu, Z., Khedher, K., and Lolli, S., "Characteristics of fine particulate matter (PM2.5) over urban, suburban, and rural areas of Hong Kong.," Atmosphere **10**(9) (2019), https://doi.org/10.3390/atmos10090496.

[9] Yang, Y., Fan, S., Wang, L., Gao, Z., Zhang, Y., Zou, H., Miao, S., Li, Y., Huang, M., Yim, S., et al., "Diurnal evolution of the wintertime boundary layer in urban Beijing, China: Insights from Doppler lidar and a 325-m meteorological tower," Remote Sensing **12**(23), 3935 (2020), https://doi.org/10.3390/rs12233935.

[10] Zong, L., Yang, Y., Xia, H., Gao, M., Sun, Z., Zheng, Z., Li, X., Ning, G., Li, Y., and Lolli, S., "Joint occurrence of heatwaves and ozone pollution and increased health risks in Beijing, China: role of synoptic weather pattern and urbanization," Atmospheric Chemistry and Physics **22**(10), 6523–6538 (2022), https://doi.org/10.5194/acp-22-6523-2022.

[11] Tosca, M., Campbell, J., Garay, M., Lolli, S., Seidel, F., Marquis, J., and Kalashnikova, O., "Attributing accelerated summertime warming in the Southeast United States to recent reductions in aerosol burden: Indications from vertically-resolved observations," Remote Sensing **9**(7), 674 (2017), https://doi.org/10.3390/rs9070674.

[12] Lolli, S., D'Adderio, L., Campbell, J., Sicard, M., Welton, E., Binci, A., Rea, A., Tokay, A., Comerón, A., Baldasano, R. B. J. M., Gonzalez, S., .Bech, J., Afflitto, N., Lewis, J., and Madonna, F., "Vertically resolved precipitation intensity retrieved through a synergy between the ground-based NASA MPLnet lidar network measurements, surface disdrometer datasets and an analytical model solution," Remote Sensing **10**(7) (2018), 10.3390/rs10071102.

[13] Lolli, S., Vivone, G., Welton, E. J., Lewis, J. R., Campbell, J. R., Sicard, M., Comeron, A., and Pappalardo, G., "Fully automated light precipitation detection from mplnet and earlinet network lidar measurements," in [EPJ Web of Conferences], **237**, EDP Sciences (2020), https://doi.org/10.1051/epjconf/202023705006.

[14] G. Pappalardo, G., Amodeo, A., Apituley, A., Comeron, A., Freudenthaler, V., Linné, H., Ansmann, A., Bösenberg, J., D'Amico, G., Mattis, I., Mona, L., Wandinger, U., Amiridis, V., Alados-Arboledas, L., Nicolae, D., Wiegner, M., "EARLINET: towards an advanced sustainable European aerosol lidar network", Atmospheric Measurement Techniques, **7** (8), 2389-2409 (2014), doi: 10.5194/amt-7-2389-2014.

[15] Lolli, S. and Di Girolamo, P., "Principal component analysis approach to evaluate instrument performances in developing a cost-effective reliable instrument network for atmospheric measurements," Journal of Atmospheric and Oceanic Technology **32**(9), 1642–1649 (2015), https://doi.org/10.1175/JTECH-D-15-0085.1.

[16] Ciofini, M., Lapucci, A., and Lolli, S., "Diffractive optical components for high power laser beam sampling," Journal of Optics A: Pure and Applied Optics 5(3), 186 (2003), doi: 10.1088/1464-4258/5/3/308.
[17] Lolli, S., Sauvage, L., Loaec, S., and Lardier, M., "EZ lidar™: A new compact autonomous eye-safe scanning aerosol lidar for extinction measurements and pbl height detection. validation of the performances against other instruments and intercomparison campaigns," Óptica Pura y Aplicada **44**(1), 33–41 (2011).
[18] Comerón, A., Muñoz-Porcar, C., Rocadenbosch, F., Rodríguez-Gómez, A., Sicard, M., "Current Research in Lidar Technology Used for the Remote Sensing of Atmospheric Aerosols," Sensors **17** (6), 1450, 1-16 (2017), doi:10.3390/s17061450.
[19] Fu, Q., Liou, K. N., "On the correlated k-distribution method for radiative transfer in nonhomogeneous atmospheres," Journal of Atmospheric Sciences, **49** (22), 2139-2156 (1992).
[20] Lolli, S., Campbell, J.R., Lewis, J.R., Gu, Y., Welton, E.J., "Fu–Liou–Gu and Corti–Peter model performance evaluation for radiative retrievals from cirrus clouds", Atmospheric Chemistry and Physics, **17**(11), 7025-7034 (2017).
[21] Kendall, M.G., [Rank correlation methods]. Charles Griffin, London, 120 (1975).